KNOWLEDGE-AIDED (POTENTIALLY COGNITIVE) SIDELOBE NULLING ON TRANSMIT FOR MECHANICAL DISTORTIONS OF PHASED ARRAY ANTENNAS

Ying Sun[*], Zishu He, and Jun Li

School of Electronic Engineering, University of Electronic Science and Technology of China, Chengdu 611731, China

Abstract—Mechanical distortions of phased array antennas make transmit pattern distort. The transmit pattern cannot be simply calibrated by compensating the position error of each element since the effect of the mechanical distortions is angle-dependent. To solve this problem, we treat the element position errors measurement as prior knowledge and propose a knowledge-aided (potentially cognitive) transmit pattern design method. When the mechanical distortions occur, the cognitive transmit pattern can still place pattern nulls in the directions of interferences while preserving the main beam response of the target of interest. The proposed method is validated by simulation results.

1. INTRODUCTION

In contrast to conventional optimum/adaptive radar in which only the receiver is optimized [14], more and more scientists and researchers shift their focus to jointly optimize the transmitter and receiver, i.e., cognitive radar [1, 17]. Radar performance improvement can be achieved through optimum design on transmitter [2–13]. Therefore, a key component of a cognitive radar system is the method by which the transmitted signal is adapted in response to information regarding the radar environment [21–23]. Guerci [15] proposed an ideal cognitive sidelobe nulling on transmit method, which places transmit antenna pattern nulls in the directions of interferences while preserving the desired main beam response.

However, there are many non-ideal factors in practice [18–20]. For example, for forward looking airborne radar, phased array antennas

are generally placed in the wingspan of airplane. Launching vibration or thermal variation leads to mechanical distortions of wingspan, and correspondingly the element position moves [16]. Such element position errors cause transmit and receive pattern distortion, which significantly degrade the estimate and detection performance of the target of interest. The element position errors introduced by mechanical distortions are dependent on angle, which make the compensation of the amplitude-phase errors of each antenna impossible. Therefore, the ideal cognitive transmit pattern is no longer practicable for mechanical distortions. To solve this problem, we treat the element position error measurements as prior knowledge and propose a knowledge-aided (potentially cognitive) transmit pattern design method. The cognitive transmit pattern can still simultaneously place pattern nulls in the directions of interferences while preserving the desired main beam response for mechanical distortions. As to the measurements of phased array antenna position error, we can obtain them through placing several tags in the surface of the antenna. Each tag transmits the dedicated signal for position measurement to the plane measure system. Then the passive system receives the dedicated signal to calculate each element position after distortion. The knowledge-aided transmit antenna pattern design is based on maximization of signal-to-interference ratio (SIR).

The paper is organized as follows. In Section 2, we introduce the position error model and analyze the effect of element position errors. In Section 3, we propose a cognitive transmit antenna pattern design method which is adapted to the element position errors. In Section 4, we present the simulation results to validate the proposed method. Finally, the conclusion is given in Section 5.

2. PROBLEM FORMULATION

Consider a narrowband M elements uniform linear array (ULA) with half wavelength interelement spacing. Due to the mechanical distortions, the ULA element position moves. The mth element positions before and after mechanic distortion are simultaneously displayed in Fig. 1.

The mth element position moves from (x_m, y_m) to $(\hat{x}_m, \hat{y}_m)$ as illustrated in Fig. 1, where the black square and red circle represent the initial position and the position after distortion, respectively, and θ is the incident direction. According to geometrical relationship in Fig. 1, we have

$$\begin{cases} \Delta x_m = \hat{x}_m - x_m \\ \Delta y_m = \hat{y}_m - y_m \end{cases} \tag{1}$$
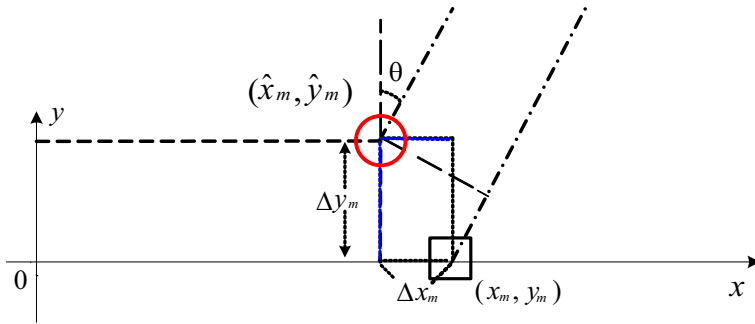
Figure 1. The mth element position change due to the mechanical distortions.

where $m = 1, 2, \ldots, M$. Due to the mechanical distortions, the wave path changes for incident direction θ. Correspondingly, the change in wave path is

$$\Delta d_m(\theta) = \Delta y_m \cos\theta + \Delta x_m \sin\theta \qquad (2)$$

Obviously, it is a function of angle of arrival (AoA). For all M elements of ULA, the change in phase can be written as

$$\mathbf{\Delta}(\theta) = [e^{j2\pi\Delta d_1(\theta)/\lambda}, e^{j2\pi\Delta d_2(\theta)/\lambda}, \ldots, e^{j2\pi\Delta d_M(\theta)/\lambda}] \qquad (3)$$

where λ is wavelength. Therefore, the mechanical distortions make the array steering vector append with a phase term:

$$\mathbf{\Gamma}(\theta) = \mathrm{diag}[\mathbf{\Delta}(\theta)] = \begin{bmatrix} e^{j2\pi\Delta d_1/\lambda} & 0 & \cdots & 0 \\ 0 & e^{j2\pi\Delta d_2/\lambda} & \cdots & 0 \\ \vdots & \vdots & \ddots & \vdots \\ 0 & 0 & \cdots & e^{j2\pi\Delta d_M/\lambda} \end{bmatrix} \qquad (4)$$

where $\mathbf{\Gamma}(\theta)$ is a $M \times M$ diagonal matrix which is angle-dependent. Hence, mechanical distortions make transmit steering vector change from

$$\mathbf{a}_T(\theta) = \left[1, e^{-j2\pi f_s(\theta)}, \ldots, e^{-j2\pi(M-1)f_s(\theta)}\right]^T \qquad (5)$$

to

$$\hat{\mathbf{a}}_T(\theta) = \mathbf{\Gamma}(\theta)\mathbf{a}_T(\theta) \qquad (6)$$

where $(\cdot)^T$ represents transpose, and $f_s(\theta)$ is spatial angle frequency. Taking forward looking airborne phased array radar as an example, spatial angle frequency is given by

$$f_s(\theta) = \frac{d \sin\theta \cos\varphi}{\lambda} \qquad (7)$$

where d is the interelement spacing of the ULA, and θ and φ stand for azimuth and elevation, respectively, where $\theta \in [-90°, 90°]$. Equation (6) implies that the transmit pattern cannot be calibrated by simple compensating the amplitude and phase of each element position error. Assume that the target of interest and the strong interferences are at the same range bin, which means that they have the same elevation, namely, $\varphi = \varphi_0$. For $\theta = (\theta_1, \theta_2, \ldots, \theta_{Nc})$, the transmit array manifold correspondingly changes from

$$\mathbf{A} = [\mathbf{a}_T(\theta_1), \mathbf{a}_T(\theta_2), \ldots, \mathbf{a}_T(\theta_{Nc})] \in \mathrm{C}^{M \times Nc} \tag{8}$$

to

$$\hat{\mathbf{A}} = [\mathbf{\Gamma}(\theta_1)\mathbf{a}_T(\theta_1), \mathbf{\Gamma}(\theta_2)\mathbf{a}_T(\theta_2), \ldots, \mathbf{\Gamma}(\theta_{Nc})\mathbf{a}_T(\theta_{Nc})] \in \mathrm{C}^{M \times Nc} \tag{9}$$

Assume $\boldsymbol{\omega}_{opt} \in \mathrm{C}^{M \times 1}$ is the transmit optimum weight vector generated by [15], then the transmit antenna pattern for mechanical distortions of phased array antenna is given by

$$\hat{\mathbf{P}} = \boldsymbol{\omega}_{opt}^H \hat{\mathbf{A}} \tag{10}$$

where $(\cdot)^H$ represents conjugate transpose. The corresponding change in transmit antenna pattern is

$$
\begin{aligned}
\Delta\mathbf{P} = \hat{\mathbf{P}} - \mathbf{P} &= \boldsymbol{\omega}_{opt}^H(\hat{\mathbf{A}} - \mathbf{A}) \\
&= \boldsymbol{\omega}_{opt}^H[(\mathbf{\Gamma}(\theta_1) - \mathbf{I})\mathbf{a}_T(\theta_1), (\mathbf{\Gamma}(\theta_2) - \mathbf{I})\mathbf{a}_T(\theta_2), \ldots, (\mathbf{\Gamma}(\theta_{Nc}) - \mathbf{I})\mathbf{a}_T(\theta_{Nc})] \\
&= \left[\sum_{m=0}^{M-1} \boldsymbol{\omega}_{opt}^*(m) \left(e^{j2\pi\Delta d_m(\theta_1)/\lambda} - 1 \right) e^{-j2\pi m f_s(\theta_1)}, \ldots, \right. \\
&\qquad \left. \sum_{m=0}^{M-1} \boldsymbol{\omega}_{opt}^*(m) \left(e^{j2\pi\Delta d_m(\theta_{Nc})/\lambda} - 1 \right) e^{-j2\pi m f_s(\theta_{Nc})} \right]
\end{aligned} \tag{11}
$$

where $(\cdot)^*$ represents conjugate. For the direction of target of interest θ_t and the K direction of interferences $\theta_k, k = 1, 2, \ldots, K$, the changes in transmit antenna patterns $\Delta\mathbf{P}(\theta_t)$ and $\Delta\mathbf{P}(\theta_k)$ are, respectively,

$$\begin{cases} \Delta\mathbf{P}(\theta_t) \neq 0 \\ \Delta\mathbf{P}(\theta_k) \neq 0, \quad i = 1, 2, \ldots, K \end{cases} \tag{12}$$

Equation (12) implies that the desired main beam response and the nulls in the direction of interferences cannot be maintained due to the phase term $e^{j2\pi\Delta d_m(\theta)/\lambda}$. Therefore, the transmit antenna pattern obtained by Equation (10) cannot achieve the desired result. To solve this problem, we propose a simple cognitive transmit pattern design method, which is adapted in response to the element position errors. The detail of the design method is given in the following section.

3. COGNITIVE TRANSMIT PATTERN DESIGN

Consider an airborne radar equipped phased array antennas. The number of transmitting antennas and number of receiving antennas are M and N, respectively. Assume that the transmit weight vector is $\hat{\boldsymbol{\omega}}$ to distinguish from $\boldsymbol{\omega}$ produced by [15]. For convenience, we still take forward looking array as an example. For the direction of the target of interest θ_t, the transmit and receive steering vectors are, respectively,

$$
\begin{aligned}
\mathbf{a}_T^t(\theta_t) &= \left[1, e^{-j2\pi d_{ET}\sin\theta_t\cos\varphi_0/\lambda}, \dots, e^{-j2\pi(M-1)d_{ET}\sin\theta_t\cos\varphi_0/\lambda}\right]^T \\
\mathbf{a}_R^t(\theta_t) &= \left[1, e^{-j2\pi d_{ER}\sin\theta_t\cos\varphi_0/\lambda}, \dots, e^{-j2\pi(N-1)d_{ER}\sin\theta_t\cos\varphi_0/\lambda}\right]^T
\end{aligned} \quad (13)
$$

where d_{ET} and d_{ER} are the interelement spacing of the transmit and receive arrays, respectively. The transmit and receive steering vectors due to mechanical distortions are modified to, respectively,

$$
\begin{aligned}
\hat{\mathbf{a}}_T^t &= \boldsymbol{\Gamma}(\theta_t)\mathbf{a}_T^t(\theta_t) \\
\hat{\mathbf{a}}_R^t &= \boldsymbol{\Gamma}(\theta_t)\mathbf{a}_R^t(\theta_t)
\end{aligned} \quad (14)
$$

The pulse compression output of the target component of the echo signal can be written as

$$
\mathbf{x}_s = \hat{\mathbf{a}}_R^t(\theta_t)\left(\hat{\mathbf{a}}_T^t(\theta_t)\right)^H \hat{\boldsymbol{\omega}} = \boldsymbol{\Gamma}(\theta_t)\mathbf{a}_R^t(\theta_t)\left[\mathbf{a}_T^t(\theta_t)\right]^H [\boldsymbol{\Gamma}(\theta_t)]^H \hat{\boldsymbol{\omega}} \quad (15)
$$

If we see the target of interest as a system, then the transmit weight vector $\hat{\boldsymbol{\omega}}$ and the pulse compression result $\mathbf{x}_s$ can be viewed as the system input and output, respectively. Then according to Equation (15), the transfer matrix $\mathbf{H}_t$ of the system is

$$
\mathbf{H}_t = \boldsymbol{\Gamma}(\theta_t)\mathbf{a}_R^t(\theta_t)\left[\mathbf{a}_T^t(\theta_t)\right]^H [\boldsymbol{\Gamma}(\theta_t)]^H \quad (16)
$$

Next, we analyze the interference component. For the direction of kth interference θ_k, the transmit and receive steering vectors are, respectively,

$$
\begin{aligned}
\mathbf{a}_T^{I_k}(\theta_k) &= \left[1, e^{-j2\pi d_{ET}\sin\theta_k\cos\varphi_0/\lambda}, \dots, e^{-j2\pi(M-1)d_{ET}\sin\theta_k\cos\varphi_0/\lambda}\right]^T \\
\mathbf{a}_R^{I_k}(\theta_k) &= \left[1, e^{-j2\pi d_{ER}\sin\theta_k\cos\varphi_0/\lambda}, \dots, e^{-j2\pi(N-1)d_{ER}\sin\theta_k\cos\varphi_0/\lambda}\right]^T, \\
&\qquad k = 1, 2, \dots, K
\end{aligned} \quad (17)
$$

Element position errors modify the kth interference's transmit and receive steering vectors from Equation (17) to

$$
\begin{aligned}
\hat{\mathbf{a}}_T^{I_k}(\theta_k) &= \boldsymbol{\Gamma}(\theta_k)\mathbf{a}_T^{I_k}(\theta_k) \\
\hat{\mathbf{a}}_R^{I_k}(\theta_k) &= \boldsymbol{\Gamma}(\theta_k)\mathbf{a}_R^{I_k}(\theta_k)
\end{aligned} \quad (18)
$$

After pulse compression, the kth interference output is

$$\mathbf{x}_{I_k} = \hat{\mathbf{a}}_R^{I_k}(\theta_k) \left(\hat{\mathbf{a}}_T^{I_k}(\theta_k) \right)^H \hat{\boldsymbol{\omega}} = \boldsymbol{\Gamma}(\theta_k) \mathbf{a}_R^{I_k}(\theta_k) \left[\mathbf{a}_T^{I_k}(\theta_k) \right]^H [\boldsymbol{\Gamma}(\theta_k)]^H \hat{\boldsymbol{\omega}} \quad (19)$$

Then, the K interferences' output is given by

$$\mathbf{x}_I = \sum_{k=1}^{K} \alpha_k \hat{\mathbf{a}}_R^{I_k}(\theta_k) \left(\hat{\mathbf{a}}_T^{I_k}(\theta_k) \right)^H \hat{\boldsymbol{\omega}}$$

$$= \sum_{k=1}^{K} \alpha_k \boldsymbol{\Gamma}(\theta_k) \mathbf{a}_R^{I_k}(\theta_k) \left[\mathbf{a}_T^{I_k}(\theta_k) \right]^H [\boldsymbol{\Gamma}(\theta_k)]^H \hat{\boldsymbol{\omega}} \quad (20)$$

where α_k represents a complex scale factor associated with the kth interference. Similarly, we see the K interferences as a system and view the transmit weight vector $\hat{\boldsymbol{\omega}}$ and the pulse compression output $\mathbf{x}_I$ as the input and output of the system, respectively. Then according to Equation (20), the transfer matrix $\mathbf{H}_I$ of the interference system is

$$\mathbf{H}_I = \sum_{k=1}^{K} \alpha_k \boldsymbol{\Gamma}(\theta_k) \mathbf{a}_R^{I_k}(\theta_k) \left[\mathbf{a}_T^{I_k}(\theta_k) \right]^H [\boldsymbol{\Gamma}(\theta_k)]^H \quad (21)$$

Then, the corresponding signal-to-interferer ratio (SIR) at the input to the receiver is given by

$$\text{SIR} = \frac{\mathbf{x}_s^H \mathbf{x}_s}{\mathbf{x}_I^H \mathbf{x}_I} = \frac{\hat{\boldsymbol{\omega}}^H \mathbf{H}_t (\mathbf{H}_t)^H \hat{\boldsymbol{\omega}}}{\hat{\boldsymbol{\omega}}^H \mathbf{H}_I (\mathbf{H}_I)^H \hat{\boldsymbol{\omega}}} \quad (22)$$

Resorting to the SIR criterion, the cognitive transmit pattern design can be formulated as the following optimization problem:

$$\max_{\hat{\boldsymbol{\omega}}} \frac{\hat{\boldsymbol{\omega}}^H \mathbf{H}_t (\mathbf{H}_t)^H \hat{\boldsymbol{\omega}}}{\hat{\boldsymbol{\omega}}^H \mathbf{H}_I (\mathbf{H}_I)^H \hat{\boldsymbol{\omega}}} \quad (23)$$

This is the well-known generalized Rayleigh quotient. The solution of $\hat{\boldsymbol{\omega}}$ is the principal component of the matrix $(\mathbf{H}_I (\mathbf{H}_I)^H)^{-1} \mathbf{H}_t (\mathbf{H}_t)^H$, and the maximum of the objective function is the corresponding eigenvector of the largest eigenvalue of $(\mathbf{H}_I (\mathbf{H}_I)^H)^{-1} \mathbf{H}_t (\mathbf{H}_t)^H$, which is denoted as $\hat{\boldsymbol{\omega}}_{opt}$.

Solving Equation (23) for optimum eigenvector yields the transmit pattern that maximizes the SIR:

$$\mathbf{P}_c = \hat{\boldsymbol{\omega}}_{opt}^H \hat{\mathbf{A}} \quad (24)$$

The transmit pattern $\mathbf{P}_c$ has the capability of placing the nulls in the directions of interferers, while preserving the desired main beam response for mechanical distortions of phased array antennas. The next section will validate the proposed method by simulation results.

4. SIMULATION RESULTS

In this section, we use the MATLAB software to simulate. The simulation process is generalized as follows: 1) Generate element positions after mechanical distortions according to the prior knowledge of element position errors. 2) Solve the Equation (23) and obtain the corresponding eigenvector of the largest eigenvalue of $(\mathbf{H}_I(\mathbf{H}_I)^H)^{-1}\mathbf{H}_t(\mathbf{H}_t)^H$ as the optimum weights $\hat{\boldsymbol{\omega}}_{opt}$. 3) Generate the cognitive transmit pattern according to Equation (24).

First of all, we consider a forward looking array airborne radar system, which is a narrowband $M = 17$ element ULA with half-wavelength interelement spacing and assume that the same ULA is used for both transmission and reception, namely, $d_{ET} = d_{ER} = \lambda/2$. At this point, the phased array antennas were placed in the wingspan of the airplane. When launching vibration or thermal variation occurs, the wingspan distorts. The element positions before and after mechanical distortions are simultaneously displayed in Fig. 2.
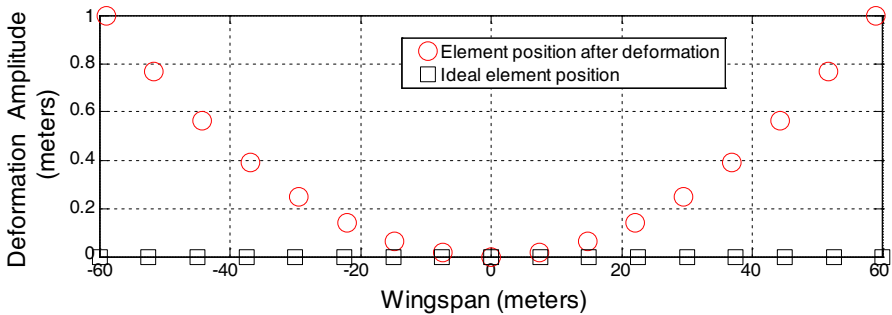

Figure 2. The distortion of wingspan for forward looking array.

For forward looking array, the simulation will be classified into two cases to perform. One is only interference, and the other is multiple interferences.

4.1. Single Interference

In addition to the desired target at $\theta_t = 0°$, there is a strong interference at $\theta_1 = 45°$ (shown as the blue star in Fig. 2). The competing interference amplitude was set to $40\,\text{dB}$ relative to the desired target, and $0\,\text{dB}$ of diagonal loading was added to $\mathbf{H}_I(\mathbf{H}_I)^H$ to improve numerical conditioning and allow for its inversion. The presence of the target and interference could have been detected
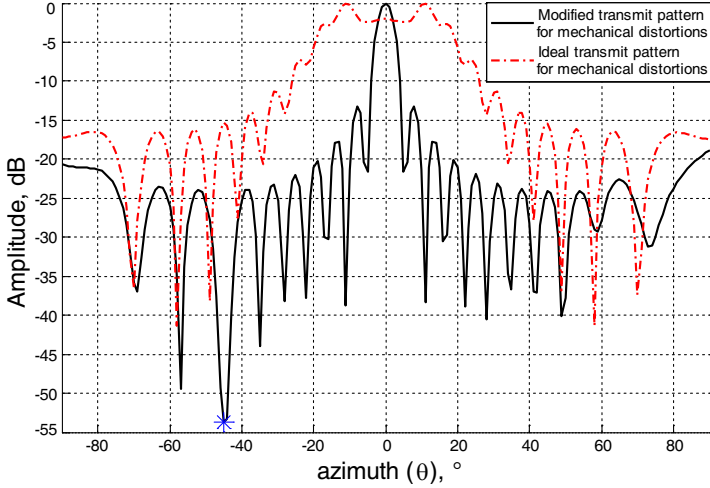
Figure 3. Comparison modified transmit pattern with ideal transmit pattern for single interference.

previously, and thus their directions known — especially if the interference was strong which is precisely the one we are concerned about since its strong sidelobes could potentially mask weaker main lobe target. With this knowledge, it is desired to minimize any energy from the interference leaking into main beam detection of the target of interest by nulling on transmit — that is by placing transmit antenna pattern nulls in the directions of the unwanted interference. The optimum transmitting weight vector $\boldsymbol{\omega}_{opt}$ obtained by [15] under ideal conditions can achieve satisfactory results [15]. However, when the wingspan is distorted according to Fig. 2, $\boldsymbol{\omega}_{opt}$ cannot yield the desired transmit pattern as shown in Fig. 3.

For transmit pattern yielded by $\boldsymbol{\omega}_{opt}$ depicted in red dashed line of Fig. 3, it does not have main beam response in the direction of the target of interest, nor has it the null in the direction of the strong interference. From the simulation result, it can be clearly understood that $\boldsymbol{\omega}_{opt}$ cannot yield a desired transmit pattern under the effect of mechanical distortions. Then we use the proposed method in this paper to obtain optimum transmit weight vector $\hat{\boldsymbol{\omega}}_{opt}$, which is adapted in response to element position errors. The modified transmit pattern for mechanical distortions is also displayed in Fig. 3. Note the presence of modified transmit pattern null in the direction of the interference while preserving the main beam response of the target of interest as desired, as depicted in solid black line of Fig. 3.

4.2. Multiple Interferences

Assume that there are strong interferences at $\theta_1 = -30°$, $\theta_2 = 10°$, $\theta_3 = 45°$, respectively, which are shown as the blue stars in Fig. 4. The desired target is at $\theta_t = 0°$. Element position errors model and all other parameters are the same as the above single interference simulation. Likewise, these directions of target and interferences and the element positions before and after the distortion are the prior information. The simulation results are shown in Fig. 4.
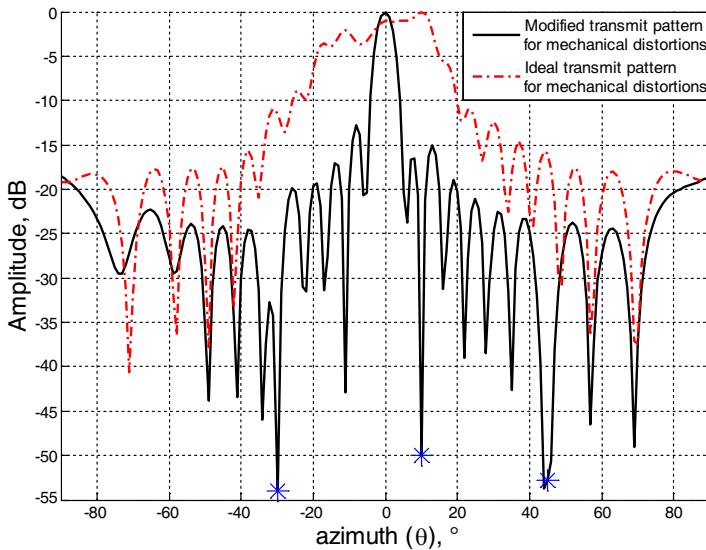

Figure 4. Comparison modified transmit pattern with ideal transmit pattern for multiple interferences.

Obviously, the transmit pattern yielded by $\hat{\boldsymbol{\omega}}_{opt}$ outperforms $\boldsymbol{\omega}_{opt}$ since the former simultaneously has nulls in these interference directions and maximum beam response in the target of interest while the latter could not.

Next, we consider the sidelooking array case. The derivation in Section 3 needs to be modified slightly. Specifically, the spatial angle frequency, namely Equation (7), is modified to

$$f_s(\theta) = \frac{d \cos \theta \cos \varphi}{\lambda} \tag{25}$$

where $\theta \in [0°, 180°]$. Assume that $M = 33$. At this point, the ULA was displayed in the fuselage, and the mechanical distortions are illustrated as in Fig. 5.
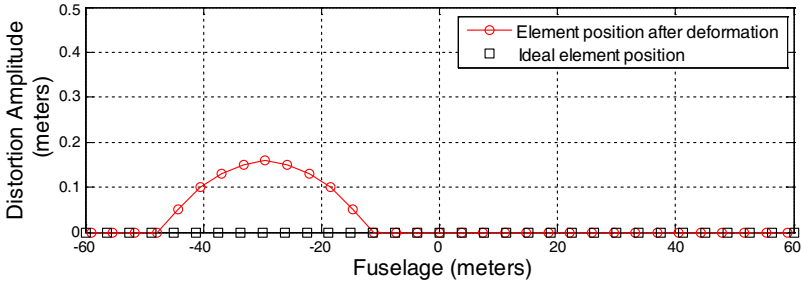
Figure 5. The mechanical distortion for sidelooking array.

For sidelooking array, the simulations are also classified into two cases to perform, namely, single interference case and multiple interferences case.

4.3. Single Interference

Except the element position errors information, the desired target direction and interference direction are also known, namely, $\theta_t = 90°$ and $\theta_1 = 165°$, where the interference direction is shown as the blue star in Fig. 6. The comparison simulation results are illustrated in Fig. 6. The proposed method is in solid black line and the ideal
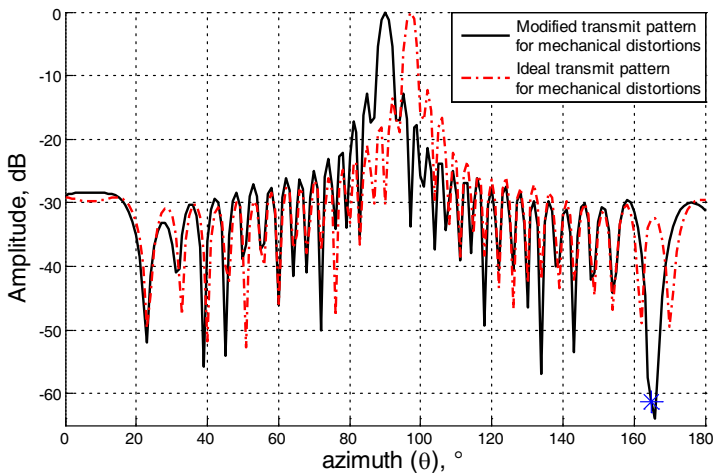

Figure 6. Comparison modified transmit pattern with ideal transmit pattern for single interference.

transmit pattern depicted in red dashed line. Obviously, modified transmit pattern achieved satisfactory result, but the ideal transmit pattern could not.

4.4. Multiple Interferences

The known prior information includes the direction of the target of interest $\theta_t = 90°$ and the directions of three strong interferences $\theta_1 = 30°$, $\theta_2 = 100°$, $\theta_3 = 145°$ (shown as the blue stars in Fig. 7). The element positions before and after the mechanical distortions are illustrated in Fig. 5. At this point, the simulation results are shown in Fig. 7.
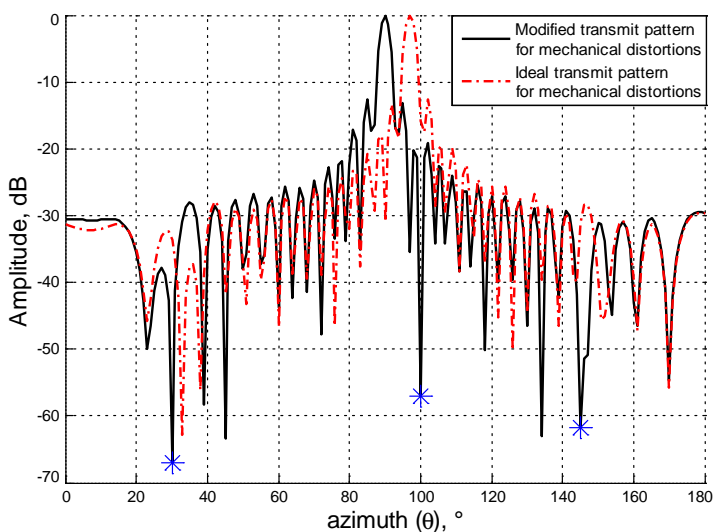

Figure 7. Comparison modified transmit pattern with ideal transmit pattern for multiple interferences.

Note the presence of modified transmit pattern nulls in the directions of the interferences as desired while preserving the main beam response of the target of interest, as depicted in solid black line of Fig. 7. Obviously, for sidelooking array case, modified transmit pattern achieved satisfactory result, but the ideal transmit pattern could not.

5. CONCLUSION

In this paper, a simple cognitive transmit pattern design method has been proposed for presenting nulls in the direction of interferences and main beam response in the direction of the target of interest for mechanical distortions. In contrast to conventional adaptive radar in which primarily the receiver is optimized, we derived the cognitive transmit pattern design method which works well in the transmitter. Although the technique given in this paper was used for transmit pattern design, it may be extended to airborne space-time transmit pattern for mechanical distortion.

ACKNOWLEDGMENT

REFERENCES

1. Haykin, S., "Cognitive radar: A way of the future," *IEEE Magazine on Signal Processing*, Vol. 23, 30–40, 2006.
2. Bergin, J. S., P. M. Techaus, J. E. Don Carlos, and J. R. Guerci, "Radar waveform optimization for colored noise mitigation," *2005 IEEE International Radar Conference*, 149–154, Washington, D.C., May 9–12, 2005.
3. Li, J., J. R. Guerci, and L. Xu, "Signal waveform's optimum-under-restriction design for active sensing," *IEEE Signal Processing Letters*, Vol. 13, 565–568, 2006.
4. Patton, L. K. and B. D. Rigling, "Modulus constraints in adaptive radar waveform design," *2008 IEEE International Radar Conference*, 1–6, Rome, Italy, May 26–30, 2008.
5. De Maio, A., S. De Nicola, Y. Huang, Z.-Q. Luo, and S. Zhang, "Design of phase codes for radar performance optimization with a similarity constraint," *IEEE Transactions on Signal Processing*, Vol. 57, 610–621, 2009.
6. De Maio, A., Y. Huang, M. Piezzo, S. Zhang, and A. Farina, "Design of optimized radar codes with a peak to average power ratio constraint," *IEEE Transactions on Signal Processing*, Vol. 59, 2683–2697, 2011.
7. Rummler, W. D., "A technique for improving the clutter performance of coherent pulse trains signals," *IEEE Transactions on Aerospace and Electronic Systems*, Vol. 3, 689–699, 1967.

8. Thompson, J. S. and E. L. Titlebaum, "The design of optimal radar waveforms for clutter rejection using the maximum principle," *Supplement to the IEEE Transactions on Aerospace and Electronic Systems*, Vol. 6, 582–589, 1967.

9. Stoica, P., H. He, and J. Li, "Optimization of the receive filter and transmit sequence for active sensing," *IEEE Transactions on Signal Processing*, Vol. 60, 1730–1740, 2012.

10. Romero, R. A. and N. A. Goodman, "Waveform design in signal-dependent interference and application to target recognition with multiple transmissions," *IEE Proceedings — Radar, Sonar and Navigation*, Vol. 3, 328–340, 2009.

11. Kay. S. M. and J. H. Thanos, "Optimal transmit signal design for active sonar/radar," *2002 IEEE Conference on Acoustic Speech, and Signal Processing (ICASSP 02)*, Vol. 2, 1513–1516, 2002.

12. Kay, S., "Optimal signal design for detection of Gaussian point targets in stationary Gaussian clutter/reverberation," *IEEE Journal of Selected Topics in Signal Processing*, Vol. 1, 31–41, 2007.

13. Kay, S., "Optimal detector and signal design for STAP based on the frequency-wavenumber spectrum," 2010, http://www.Ele.uri. Edu/faculty/kay/New%20web/downloadable%20files/STAP_signal_design_AFOSR.pdf.

14. Guerci, J. R., "Theory and application of covariance matrix tapers for robust adaptive beamforming," *IEEE Transcations on Signal Processing*, Vol. 47, 977–985, 1999.

15. Guerci, J. R., *Cognitive Radar: The Knowledge-aided Fully Adaptive Approach*, Artech House, Boston/London, 2010.

16. Takahshi, T., N. Nakamoto, M. Ohtsuka, T. Aoki, Y. Konishi, and M. Yajima, "A simple on-board calibration method and its accuracy for mechanical distortions of satellite phased array antennas," *EuCAP*, 1573–1577, 2009.

17. Aubry, A., A. DeMaio, A. Farina, and M. Wicks, "Knowledge-aided (potentially cognitive) transmit signal and receive filter design in signal-dependent clutter," *IEEE Transactions on Aerospace and Electronic System*, Vol. 49, 93–117, 2013.

18. Keydel, W., "Perspectives and visions for future SAR systems," *IEE Radar Sonar Navigation*, Vol. 150, 97–103, 2003.

19. Wang, H. S. C., "Performance of phased-array antennas with mechanical errors," *IEEE Transactions on Aerospace and Electronic Systems*, Vol. 28, 535–545, 1992.

20. James, K., D. Peterman, and V. Glavac, "Distortion measurement

and compensation in a synthetic aperture radar phased-array antenna," *2010 14th International Symposium on Antenna Technology and Applied Electromagnetics and the American Electromagnetics and the American Electromagnetics Conference*, 978–982, 2010.

21. Maity, D., U. Halder, and S. Das, "An informative differential evolution algorithm with self adaptive re-clustering technique for the optimization of phased antenna array," *Progress In Electromagnetics Research B*, Vol. 40, 361–380, 2012.

22. Li, W.-T., X.-W. Shi, and Y.-Q. Hei, "An improved particle swarm optimization algorithm for pattern synthesis of phased arrays," *Progress In Electromagnetics Research*, Vol. 82, 319–332, 2008.

23. Eldek, A. A., "Design of double dipole antenna with enhanced usable bandwidth for wideband phased array applications," *Progress In Electromagnetics Research*, Vol. 59, 1–15, 2006.